Microwave plasma discharges for biomass pretreatment: Degradation of a sodium carboxymethyl cellulose model

Cite as: AIP Advances 10, 095025 (2020); doi: 10.1063/5.0018626
Submitted: 16 June 2020 • Accepted: 27 August 2020 •
Published Online: 22 September 2020

B. Honnorat,[a] V. Brüser, and J. F. Kolb

AFFILIATIONS

Leibniz Institute for Plasma Science and Technology (INP), Felix-Hausdorff-Str. 2, D-17489 Greifswald, Germany

[a]Author to whom correspondence should be addressed: bruno.honnorat@gmail.com

ABSTRACT

Biogas production is an important component of an environmentally benign renewable energy strategy. However, the cost-effectiveness of biogas production from biomass is limited by the presence of polymeric structures, which are recalcitrant to digestion by bacteria. Therefore, pretreatments must often be applied prior to anaerobic fermentation to increase yields of biogas. Many physico-chemical pretreatments have a high energy demand and are generally costly. An alternative could be the ignition of a plasma directly in the biomass substrate. The reactive species that are generated by plasma–liquid interactions, such as hydroxyl radicals and hydrogen peroxides, could contribute significantly to the disintegration of cell walls and the breakage of poorly digestible polymers. With respect to economic, processing, and other potential benefits, a microwave instigated and sustained plasma was investigated. A microwave circuit transmitted 2-kW pulses into a recirculated sodium carboxymethyl cellulose solution, which mimicked the rheological properties of biomass. Each microwave pulse had a duration of 12.5 ms and caused the ignition of a discharge after a vapor bubble had formed. Microwaves were absorbed in the process with an efficiency of ~97%. Slow-motion imaging showed the development of the discharge. The plasma discharges provoked a decrease in the viscosity, probably caused by the shortening of polymer chains of the cellulose derivative. The decrease in viscosity by itself could reduce processing costs and promotes bacterial activity in actual biomass. The results demonstrate the potential of microwave in-liquid plasma discharges for the pretreatment of biomass.

Biogas is a renewable source of energy that could play a key role in the energy transition.[1] The gas is mainly a mixture of CH_4, CO_2, and H_2 produced during the anaerobic digestion of biomass by a consortium of bacteria.[2] The environmental benefit of biogas includes the replacement of natural gas, fossil fuels, and the reduction of greenhouse gas emissions from landfills.[1,3] The digestion of biomass is a four-phase process,[4] which degrades long and complex polymeric chains into biogas. The first step, polymer hydrolysis, limits the kinetic of the reaction[5] for the most recalcitrant substance, such as lignocellulose.[5,6] Especially, animal manures contain a high proportion of lignocellulose and are poorly digestible without physical or chemical pretreatments[5] that facilitate degradation.

However, most pretreatments are energy-intensive and require harsh conditions. For example, steam-explosion pretreatments involve heating over 100 °C and high-pressure conditions.[5] Other technologies imply the addition of corrosive chemicals, such as nitric acid, alkali solutions, concentrated hydrogen peroxide, or ozone,[4] in combination with heating.[4,5]

Consequently, new pretreatment methods are highly in demand, and plasma is hereby a promising candidate. Plasma can be produced in DC,[7] radio frequency,[8,9] microwave,[10] or ns-pulsed[11] discharges. The plasma–liquid interaction produces highly reactive chemical species[11] in the liquid phase, such as hydroxyl radical and H_2O_2. The main advantage of plasma over other pretreatments would be the possibility of generating these strong oxidizing agents from the biomass itself without the environmental and economic costs of externally supplied chemicals.

The generation of plasma in water[2,13] and organic solvents[10] has already been demonstrated, and plasma–liquid interactions have been investigated for the degradation of noxious chemical

compounds[12,13] and cellulose or glucose for the purpose of hydrogen production.[14,15] Ignition of plasma is generally facilitated by the injection of argon bubbles in the presence of radio frequency or microwave electric fields.[16,17] Neither the use of a noble gas nor air are acceptable for biomass treatment. Noble gases are economically not feasible, and oxygen would prevent the anaerobic digestion of biomass.[3] Alternatively, plasma ignition can also be facilitated by reducing pressure exploiting a Venturi effect[18] or by vacuum pumping.[19,20] Such techniques are energy- and cost-intensive or not convenient because the biomass contains a significant quantity of fibers and solid particles (~cm).

So far, plasma formation in biomass, or generally in a flowing viscous liquid, at atmospheric pressure has not been investigated. Instead, research has rather focused on conditions that are not practical for the treatment of biomass, i.e., static and low-pressure conditions. Reduced pressures have also been proposed as a strategy to mitigate electrode erosion in discharge systems.[13] Other suggested methods are the protection of tungsten electrodes by a layer of heat resistant ceramic[21] or the use of microwave pulses.[22] However, economic considerations, with respect to power that can be delivered in the kilowatt range, were the primary reason for the study of microwave discharges instead of radio frequency or ns-pulsed discharges. Two characteristics were particularly examined: (a) the efficiency of the energy transfer and (b) the effect of plasma treatment on the viscosity of the model substrate.

The viscosity of biomass ranges from moderately viscous (η = 10 mPa s–1000 mPa s) to almost solid according to the percentage of dry matter.[23] As a model for biomass, an aqueous solution of sodium carboxymethyl cellulose (NaCMC) had been previously established.[24–26] NaCMC mimics the non-Newtonian rheology of biomass with adjustable viscosity. NaCMC solutions are non-toxic and transparent, which enables the direct observation of the plasma. The samples were prepared by dissolving 258 g of NaCMC (Chempoint, Walocel-CRT 30000-GA) in 60 l of tap water with vigorous stirring for 20 min. Altogether 767 g of NaCl were dissolved afterward, leading to a viscous solution ($\eta = 82 \pm 2$ mPa s) of electrical conductivity $\sigma = 22 \pm 0.5$ mS cm^{-1}. The chosen parameters are based on measurements on actual biomass that is processed by a local biogas plant.

Plasma–liquid experiments were carried out in a 3D-printed PETG reactor (Fig. 1). NaCMC solutions were circulated from the 60-l tank to the reactor and back by a pump (Ebara, Best-one-Vox-1741108300). The flow rate of 1.7 l s^{-1} was measured with a Doppler flowmeter (UFD5500, Micronics) and was similar to those used in the biogas plant. A second hydraulic circuit, consisting of a cooling coil and a temperature regulator (Easitemp 6/95, Single), maintained the temperature of the NaCMC solution below 30 °C. Temperature and conductivity were measured with a conductivity meter (FiveGo F3, Mettler Toledo).

The microwave source was a magnetron (GMP-20-KED, SAIREM), delivering 1950 W at 2.45 GHz into WR340-waveguides. A pulse generator (FY3200S, Feeltech) enabled us to command the microwave source and define the properties of the microwave pulses emitted by the magnetron. The microwave pulses are characterized by their instantaneous power, P_i, their frequency, f_r, and their duty ratio, d_r. Plasma was formed for the following parameters: f_r = 20 Hz, d_r = 25%, and P_i = 1950 W.

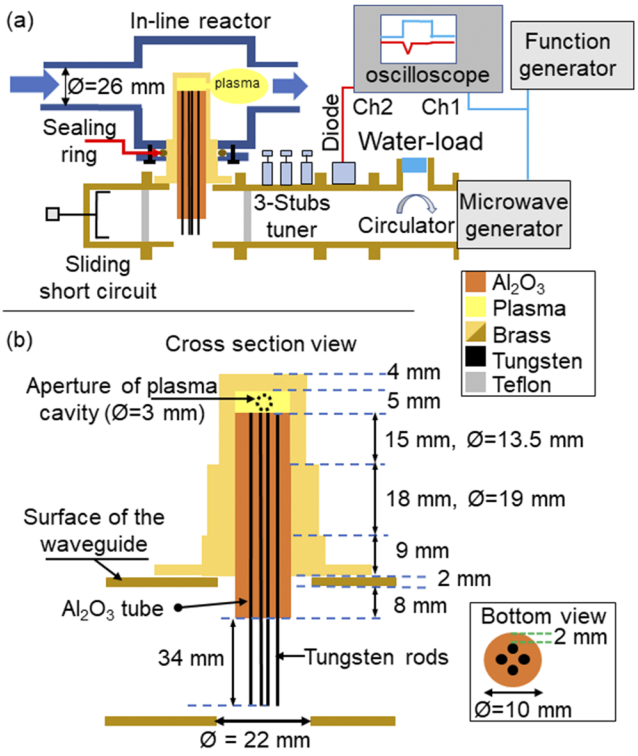

FIG. 1. Schematic of the experimental setup. The plasma was formed from the gas given by the vaporization of the liquid contained in plasma cavity. (a) Components of the microwave circuit. (b) Dimensions and relative positions of ceramic, tungsten, and brass in WR340 waveguide.

Consequently, each pulse had a length of 12.5 ms and conveyed 24.4 J. The microwave circuit included a circulator, protecting the magnetron from the reflected power (Fig. 1), a forward and reflected power measurement unit, and two tuning components: a sliding short-circuit and a 3-stubs tuner. The measuring diodes produced signals proportional to the forward and reflected power that were both recorded with an oscilloscope (WaveSurfer 64MXs-B-600 MHz, Lecroy) and processed with MATLAB (R2018b, MathWorks, Inc.). The diodes were calibrated with a vector network analyzer (ZVRE, Rhodes and Schwarz, 1043.009). The tuning components permitted us to minimize the reflected power and optimize the energetic yield of the treatment.

The function of the microwave coupler was to transmit power from the inside of the waveguide to the outside into the NaCMC solution (Fig. 1). Two 1-cm thick PTFE-windows protected the magnetron from inner-waveguide discharges. The outer conductor of the coupler is made of brass and had two holes of 10 mm and 3 mm in diameter, respectively. A 10-mm diameter, 52-mm length, Al_2O_3-tube (99.7% purity, ALM102FOUR, Almath Crucibles) was partially inserted in the brass part, leaving a 5-mm thick cavity above the ceramic tube. The Al_2O_3-tube had four boreholes with a diameter of 2 mm in which tungsten rods of length 86 mm were inserted. The microwave propagated in Al_2O_3, and the plasma was formed

between the surface of the ceramic and the metallic surface on the opposite side of the cavity. The plasma expanded freely into the flow through the sideway 3-mm hole. The microwave power, which was not absorbed by the plasma, was reflected and propagated through the plasma again. Such a structure, called Fabry–Perot plasma resonator,[27] increased the proportion of microwave power absorbed in the plasma.

Imaging was performed perpendicular to the direction of the flow of the substrate using a slow-motion camera (Chronos 1.4, Kron Technologies, Inc.) and a computar 12.5 mm–75 mm f/1.2 zoom lens. The frequency of acquisition and the exposure time were 15 941 Hz and 58 μs, respectively. Images were processed with ImageJ.[28]

Before each experiment, the solution was circulated through the hydraulic circuit for 20 min. Aliquots of 1 l were taken after 0 min, 5 min, 10 min, 15 min, 20 min, 30 min, 40 min, 50 min, 60 min, and 70 min and stored in PET bottles at ambient temperature. The samples were left to degas for 24 h. The viscosity was measured with a rotational viscosimeter (NDJ-5S, spindle No. 1).

The proportion of the forward microwave power reflected during one pulse is represented in Fig. 2(a). The reflected energy per pulse, E_b, was calculated for each acquisition (numerical integration). The mean value of E_b, $\langle E_b \rangle$ = 0.8 ± 0.3 J(N = 7378) corresponded to 3.1 ± 1.3% of the forward power. The histogram for E_b revealed that the most probable reflected energy per pulse was in the bin 0.55 J–0.6 J [Fig. 2(b)]. It was observed that the distribution of the reflected energies did not evolve over time after the discharges had reached a steady-state within ~10 s.

The stochastic behavior of the reflected power over time is shown in Fig. 2(d). The average for all the acquired signals (N = 7378) exhibited two maxima [Fig. 2(d), red line]. The maximum at t = 0 was caused by the initial mismatch between the microwave circuit and the load. Indeed, the reflected power cannot be minimized at all times since phase transitions to the gaseous and plasma state modify the electrical permittivity of the load and, thus, its reflective properties. Within the first millisecond, the substrate was vaporized, and plasma had formed. The second maxima resulted probably from the superposition of the stochastically occurring reflections.

Fourier transform analysis and continuous wavelet transform[29] (CWT) were performed with MATLAB to characterize the frequency content of the signals [Figs. 2(c) and 2(e)]. According to

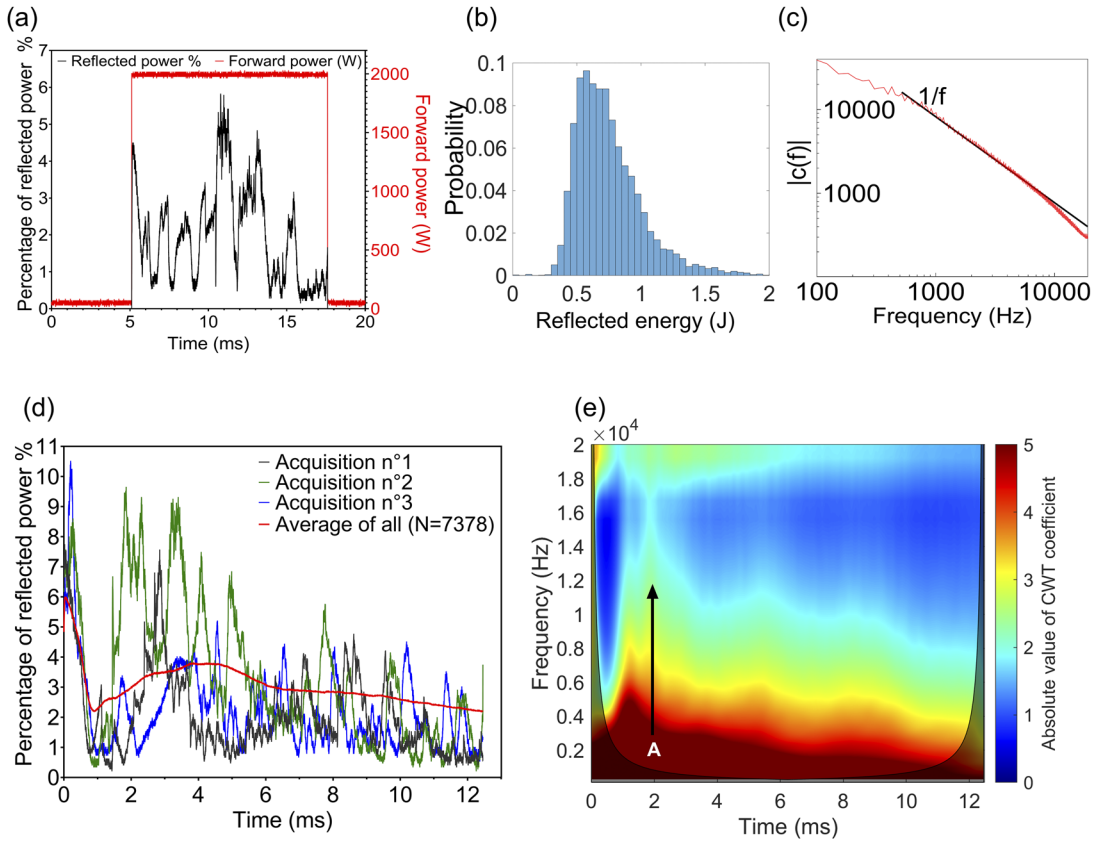

FIG. 2. Characterization of the forward and reflected power. (a) Forward microwave power (red line) and percentage of reflected power (black line). (b) Histogram of the reflected energy per pulse with the probability normalized to unity. (c) Amplitude of the coefficient of the Fourier transform. (d) Three examples for waveforms of reflected power and the averaged signal (red) for all 7378 acquisitions. (e) Absolute value of the coefficient of the continuous wavelet transform averaged over all waveforms. Event A is associated with plasma ignition. The shaded region represents the cone of influence[29] of CWT in which the signal is not interpretable.

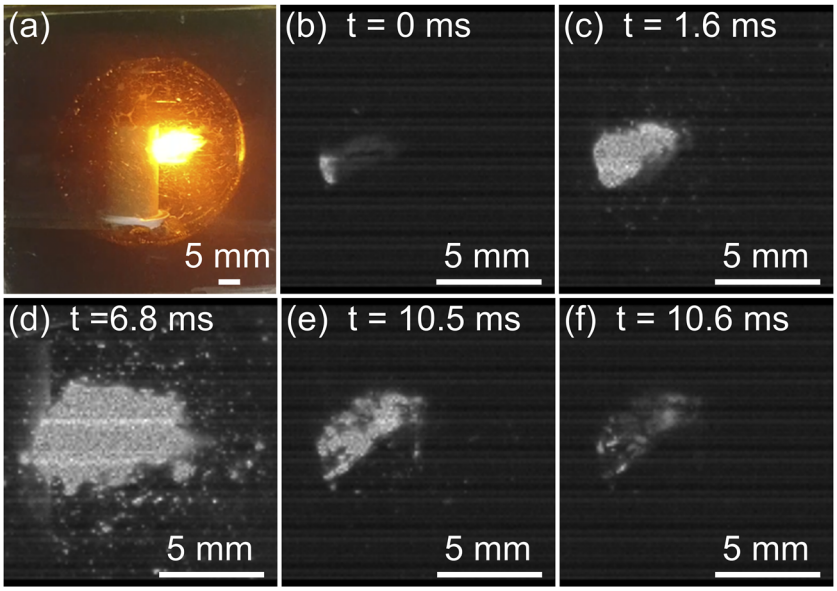

FIG. 3. Images of the microwave discharge in NaCMC solutions flowing from left to right. (a) Time integrated photograph (~15 ms) of the discharge. [(b)–(f)] Successively acquired images of one discharge with the slow-motion camera (f_r = 20 Hz, d_r = 25%, and P_i = 1950 W).

the bandwidth of the measurement system, coefficients beyond 20 kHz are not represented. The average of the magnitude of the coefficient of the CWT is plotted in Fig. 2(e). Event A was associated with the plasma ignition: a fast change in the reflected signal due to a change in the dielectric properties. The amplitude of the coefficients of the Fourier transform has a 1/f-dependency, the same as Brownian noise. This is consistent with the hypothesis of a stochastic behavior, except for the first ignition (event A).

Figure 3(a) provides a time-integrated photograph of a typical microwave discharge. Figure 3(b) is the first image from the slow-motion imaging showing the onset of a plasma defines the reference time t = 0. In the last image showing a plasma [Fig. 3(f), t = 10.6 ms], there was a substantial decrease in the luminosity compared with the previous acquired image [Fig. 3(e), t = 10.5 ms]. Consequently, at t = 10.5 ms, the end of the microwave pulse was assumed. Therefore, we deduced that 2 ms were necessary to vaporize the liquid and ignite the plasma since the length of the actual microwave pulse was 12.5 ms. Accordingly, images (b)–(e) describe the expansion of the discharge in the liquid flow.

The plasma-treated samples showed a tremendous reduction of the viscosity, η, as a function of treatment time (Fig. 4, replicates 1–3). The viscosity decreased linearly as long as η remained above 50 mPa s and then at a slower rate. The slope of the linear fit was -1.6 ± 0.4 mPa s min^{-1}. The viscosity drops below the detection limit (<15 mPa s) for longer processing times. Since the duty ratio was 25%, the average forward microwave power was 487.5 W. We defined the energetic yield, Y, of the process as the ratio of the slope of the linear part of the drop in viscosity divided by the average forward power: $Y = -3.3 \pm 0.8\ \mu\text{Pa s min}^{-1}\ \text{W}^{-1}$. No significant changes in pH values and conductivity were observed.

Pulses parameters (f_r = 1000 Hz, d_r = 12%, and P_i = 1950 W) were used to determine if the vaporization and the heating alone, i.e., without plasma ignition, could decrease the viscosity. No significant decrease in η was observed (Fig. 4, control). In addition, 20 l of NaCMC solution were heated at 50 °C for 1 h using the temperature regulator but no change in viscosity was measurable. Therefore, the decrease in viscosity is probably caused by the breaking of the polymer chains[24,30] of NaCMC. This could be due to the chemical and/or thermal conditions specific to plasma–liquid interactions.

Microwave driven discharges in a highly viscous liquid were investigated as a model for the treatment of biomass. The microwave circuit transmitted electromagnetic energy with high efficiency since 97% of the provided power was absorbed despite phase transitions and associated changes in electrical permittivity. A tremendous decrease in the viscosity was observed as a result of the

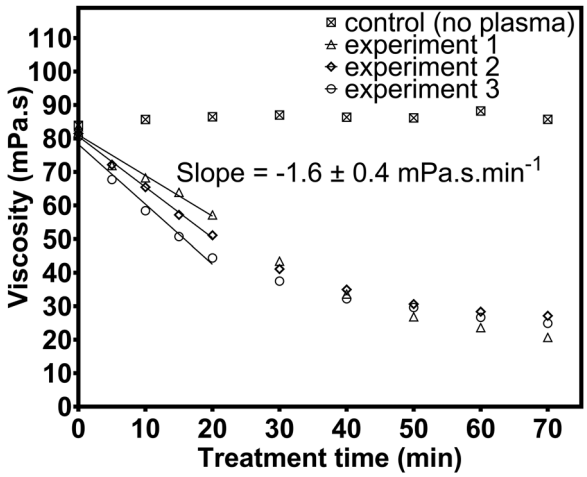

FIG. 4. Viscosity of NaCMC solutions for increasing treatment times. Three independent experiments were conducted. The mean value of the slopes was determined by linear regression analysis.

plasma exposure. Heating alone did not lead to a drop in viscosity. A possible mechanism is the breakage of polymer chains due to plasma-chemical degradation processes together with locally high temperatures. Regarding the treatment of actual biomass, a viscosity drop caused by the plasma would reduce the processing costs and the polymer breakage could increase the yield in biogas production. Processing of biomass samples and the understanding of the mechanism that are responsible for viscosity drop, such as the production of reactive species and plasma-bubble dynamics, will be investigated in future studies. The results so far already suggest a possibility for plasma to improve the biogas production and contribute to the transition toward more sustainable energy production.

The technical assistance of Tilo Schultz and Raphael Rataj is greatly appreciated. This research has been supported by the European Regional Development Fund (Grant No. TBI-V-247-VBW-086).

DATA AVAILABILITY

The data that support the findings of this study are available from the corresponding author upon reasonable request.

REFERENCES

[1] IPCC, *Climate Change 2014: Mitigation of Climate Change; Working Group III Contribution to the Fifth Assessment Report of the Intergovernmental Panel on Climate Change*, edited by O. Edenhofer (Cambridge University Press, New York, NY, 2014).

[2] S. P. Gilmore, T. S. Lankiewicz, S. E. Wilken, J. L. Brown, J. A. Sexton, J. K. Henske, M. K. Theodorou, D. L. Valentine, and M. A. O'Malley, ACS Synth. Biol. **8**, 2174 (2019).

[3] A. Wellinger, J. Murphy, and D. Baxter, *The Biogas Handbook: Science, Production and Applications* (Woodhead Publishing, 2013).

[4] M. Turco, A. Ausiello, and L. Micoli, *Treatment of Biogas for Feeding High Temperature Fuel Cells: Removal of Harmful Compounds by Adsorption Processes*, 1st ed. (Springer International Publishing, 2016).

[5] S. R. Paudel, S. P. Banjara, O. K. Choi, K. Y. Park, Y. M. Kim, and J. W. Lee, Bioresour. Technol. **245**, 1194 (2017).

[6] J. K. Saini, R. Saini, and L. Tewari, 3 Biotech **5**, 337 (2015).

[7] G. Saito, Y. Nakasugi, and T. Akiyama, J. Appl. Phys. **118**, 023303 (2015).

[8] T. Maehara, H. Toyota, M. Kuramoto, A. Iwamae, A. Tadokoro, S. Mukasa, H. Yamashita, A. Kawashima, and S. Nomura, Jpn. J. Appl. Phys., Part 1 **45**, 8864 (2006).

[9] T. Maehara, I. Miyamoto, K. Kurokawa, Y. Hashimoto, A. Iwamae, M. Kuramoto, H. Yamashita, S. Mukasa, H. Toyota, S. Nomura, and A. Kawashima, Plasma Chem. Plasma Process. **28**, 467 (2008).

[10] Y. A. Lebedev, High Temp. **56**, 811 (2018).

[11] I. Adamovich, S. D. Baalrud, A. Bogaerts, P. J. Bruggeman, M. Cappelli, V. Colombo, U. Czarnetzki, U. Ebert, J. G. Eden, P. Favia, D. B. Graves, S. Hamaguchi, G. Hieftje, M. Hori, I. D. Kaganovich, U. Kortshagen, M. J. Kushner, N. J. Mason, S. Mazouffre, S. M. Thagard, H.-R. Metelmann, A. Mizuno, E. Moreau, A. B. Murphy, B. A. Niemira, G. S. Oehrlein, Z. L. Petrovic, L. C. Pitchford, Y.-K. Pu, S. Rauf, O. Sakai, S. Samukawa, S. Starikovskaia, J. Tennyson, K. Terashima, M. M. Turner, M. C. M. van de Sanden, and A. Vardelle, J. Phys. D: Appl. Phys. **50**, 323001 (2017).

[12] S. Horikoshi and N. Serpone, RSC Adv. **7**, 47196 (2017).

[13] A. Tsuchida, T. Shimamura, S. Sawada, S. Sato, N. Serpone, and S. Horikoshi, Radiat. Phys. Chem. **147**, 53 (2018).

[14] F. Syahrial, K. Tange, S. Nomura, S. Mukasa, and H. Toyota, J. Jpn. Inst. Energy **96**, 451 (2017).

[15] K. Tange, S. Nomura, S. Mukasa, H. Toyota, and F. Syahrial, J. Jpn. Inst. Energy **95**, 1105 (2016).

[16] H. Aoki, K. Kitano, and S. Hamaguchi, Plasma Sources Sci. Technol. **17**, 025006 (2008).

[17] A. Hamdan, J. Profili, and M. S. Cha, Plasma Chem. Plasma Process. **40**, 169 (2020).

[18] M. Ito, T. Takahashi, S. Takitou, S. Takashima, N. Nomura, T. Kitagawa, and H. Toyoda, Jpn. J. Appl. Phys., Part 1 **56**, 026201 (2017).

[19] T. Ishijima, H. Hotta, H. Sugai, and M. Sato, Appl. Phys. Lett. **91**, 121501 (2007).

[20] T. Ishijima, K. Nosaka, Y. Tanaka, Y. Uesugi, Y. Goto, and H. Horibe, Appl. Phys. Lett. **103**, 142101 (2013).

[21] Y. Hattori, S. Mukasa, H. Toyota, H. Yamashita, and S. Nomura, Surf. Coat. Technol. **206**, 2140 (2012).

[22] S. Horikoshi, S. Sawada, S. Sato, and N. Serpone, Plasma Chem. Plasma Process. **39**, 51 (2019).

[23] D. J. Klingenberg, T. W. Root, S. Burlawar, C. T. Scott, K. J. Bourne, R. Gleisner, C. Houtman, and V. Subramaniam, Biomass Bioenergy **99**, 69 (2017).

[24] F. Conti, L. Wiedemann, M. Sonnleitner, and M. Goldbrunner, New J. Chem. **42**, 1099 (2018).

[25] N. Eshtiaghi, S. D. Yap, F. Markis, J.-C. Baudez, and P. Slatter, Water Res. **46**, 3014 (2012).

[26] L. Wiedemann, F. Conti, T. Janus, M. Sonnleitner, W. Zörner, and M. Goldbrunner, Chem. Eng. Technol. **40**, 238 (2017).

[27] C. M. Ferreira and M. Moisan, *Microwave Discharges: Fundamentals and Applications* (Springer Science & Business Media, 2013).

[28] J. Schindelin, I. Arganda-Carreras, E. Frise, V. Kaynig, M. Longair, T. Pietzsch, S. Preibisch, C. Rueden, S. Saalfeld, B. Schmid, J.-Y. Tinevez, D. J. White, V. Hartenstein, K. Eliceiri, P. Tomancak, and A. Cardona, Nat. Methods **9**, 676 (2012).

[29] C. Torrence and G. P. Compo, Bull. Am. Meteorol. Soc. **79**, 61 (1998).

[30] A. Charlesby, J. Polym. Sci. **15**, 263 (1955).